A critical assessment of the reliability of predicting subsidence phenomena induced by hydrocarbon production

A critical assessment of the reliability of predicting subsidence phenomena induced by hydrocarbon production

Angelo Cannata[a], Andrea Gotta[a], Vera Rocca[a]*

[a] Department of Environment, Land and Infrastructure Engineering, Faculty of Engineering, Politecnico di Torino, Corso Duca degli Abruzzi 24, 10129 Torino, Italy

* Correspondence: vera.rocca@polito.it; Tel.: +39-011-090-7610

Declarations of interest: none

Keywords: pseudo-elastic moduli; decay curve; subsidence analysis; medium depth clastic reservoir.

Abstract

Predictive analysis of the spatial and temporal evolution of the subsidence induced by hydrocarbon exploitation could be affected by a high uncertainty also related to the *a priori* identification of the most realistic deformation parameter values. In fact, deformation behaviour of the involved formations is not constant but evolves according to the increasing strain caused by fluid pressure drop. Especially shallow medium depth clastic formations (which contain most of the reserves in the largest known reservoirs) could exhibit an important non-linear influence of strain on formation stiffness.

The scope of this research is to provide insight into how reliable the prediction of the subsidence could be as a function of adopted pseudo-elastic values related to the non-linear poro-elastic behaviour of clastic formations. To this end, a series of multi-variable sensitivity analyses were developed to quantify the discrepancy in subsidence forecast deriving from the assumption of constant (static or dynamic) pseudo-elastic parameters values along all reservoir production life instead of inputting into the model a decay curve, which describes the progressive degradation of the pseudo-elastic parameters. The case study, even if synthetic, is a compound of standard features representative of gas-production from a clastic reservoir so as to analyse the response of a macro category.

The results of all the analysed scenarios (which differ in terms of reservoir depth, Gas Originally in Place and shape factor) allow the identification of the reference confidential intervals of static and dynamic assumptions vs the decay curve hypothesis. Furthermore, they show that even if the mechanical response of the reservoirs evolves towards the static modulus during production, the relative induced subsidence is approximated with higher accuracy by the constant dynamic modulus assumption. The results of the sensitivity analysis on synthetic models were validated via the analysis of a real gas reservoir.

1 Introduction

Hydrocarbon production as well as the storage of natural gas in underground formations require accurate safety analyses, including the evaluation of induced subsidence to assess its potential impact on existing constructions and infrastructures, especially on highly urbanized area [1-3]. In the case of predominant non-linear poro-elastic behaviour, a key role in subsidence prediction, via both analytical, semi analytical or numerical approaches, is played by the pseudo-elastic parameters. As it is well known, their values are closely related not only to the nature and the structure of the porous media, its saturated fluids and the *in situ* conditions, but it is also closely dependent on factors like strain amplitude and scale effects [4] . In particular, the strain amplitude induced into a reservoir by hydrocarbon exploitation changes as a function of the fluid pressure variation and it represents one of the system unknowns. As a best practice of the oil industry[5], subsidence forecast studies are tackled with sensitivity analysis approach thus considering constant static or dynamic pseudo-elastic parameter values, which correspond to the worst and the best scenarios, respectively. The standard nomenclature defines "static moduli" – E_{stat} as the values obtained from stress and strain measurements in a rock mechanical test and the "dynamic moduli" – E_{dyn} as the ones obtained from acoustic velocities data[6]. The latter better represents the material deformation behaviour at small strains; the first is associated with increasing strain levels. In

medium to poor consolidated rocks, particularly, the difference between static and dynamic values can be of an order of magnitude or more [4]. Needless to say, greater the uncertainty in the input model parameters, larger the confidence interval of the results (i.e. extension and magnitude of the subsidence cone). Furthermore, the use of constant pseudo-elastic parameter values along the production life of the reservoir represents an approximation to the real system deformation behaviour of which the effects on subsidence phenomena forecast should be assessed. The issue may be addressed by adopting a decay curve as the input deformation parameter: as it will be explained in detail later on, it is a transition curve describing the degradation of pseudo-elastic parameters, from dynamic to static values, as a function of the induced strain amplitude. The idea of using decay curves comes from the geotechnical field; however it is still widely ignored by the oil industry also because its empirical determination is not a trivial task.

The scope of the research presented in this paper is to quantify the reliability of subsidence phenomena prediction as a function of adopted pseudo-elastic values related to the non-linear poro-elastic behaviour of clastic formations (which contain most of the reserves in the largest known reservoirs [7,8]. To this end, a series of subsidence analyses via integrated static, dynamic and geomechanical 3D numerical approach [9-16] was performed to assess the discrepancy between results obtained assuming constant (static or dynamic) pseudo-elastic parameters values throughout reservoir production life instead of inputting into the model a decay curve. The focus of the investigation was the Italian Po Plain-Adriatic Foredeep, where the greatest Italian concentration of biogenic gas deposits is located. The choice was based on the following considerations:

1) Po Plain gas-bearing formations are generally in clastic sequences (silty to shaley sequence intercalated with arenaceous banks) characterized by substantial discrepancy between static and dynamic pseudo-elastic parameters values, as has been described by experimental evidence [17,18];
2) two coherent and complete geomechanical datasets (i.e. deformation and strength parameters) from two clastic gas-bearing formations located in the Po Plain were available and adopted for model characterization;
3) this area has been widely investigated and characterized since the early 1950s, when numerous hydrocarbon fields were discovered. In particular, for the research herein described, basic information about the Po Plain and the Adriatic Basin environmental has been taken from Benetatos et al [19]. They collected and categorized information regarding the structural, geometric, lithological, petrophysical and mechanical characteristics of nearly 250 Italian hydrocarbon fields together with data related to their production history, (when available).

In addition, the research investigated the effects of geometrical reservoir features (depth, dimension also in terms of Gas Originally In Place – GOIP and shape factor) on the production-related subsidence for each of the geomechanical configurations (constant static or dynamic pseudo-elastic parameters and the decay curve).

2 Decay curve: theoretical overview

There are a good numbers of researchers [20-23] who agreed that “one of the major problems in ground engineering in the 1970s and earlier was the apparent difference between the stiffness of soils measured in laboratory tests and those back-calculated from observation of ground movements". Despite all the technological progresses since then, the sentence still holds true actual not only for ground engineering but for hydrocarbon exploitation field as well. In fact, mechanical behaviour of clastic formations at shallow - medium depths which hold hydrocarbon reservoirs could lie between rock mechanics and soil mechanics and, during depletion, they could exhibit an important non-linear influence of the strain on the formation stiffness. As has been corroborated over the years [24-28], the maximum strain at which soils exhibit almost fully recoverable behaviour is found to be very small; then, with increasing strain, soil stiffness decays non-linearly, according to the well know semi-logarithmic reduction or decay curve (Fig. ***3***).

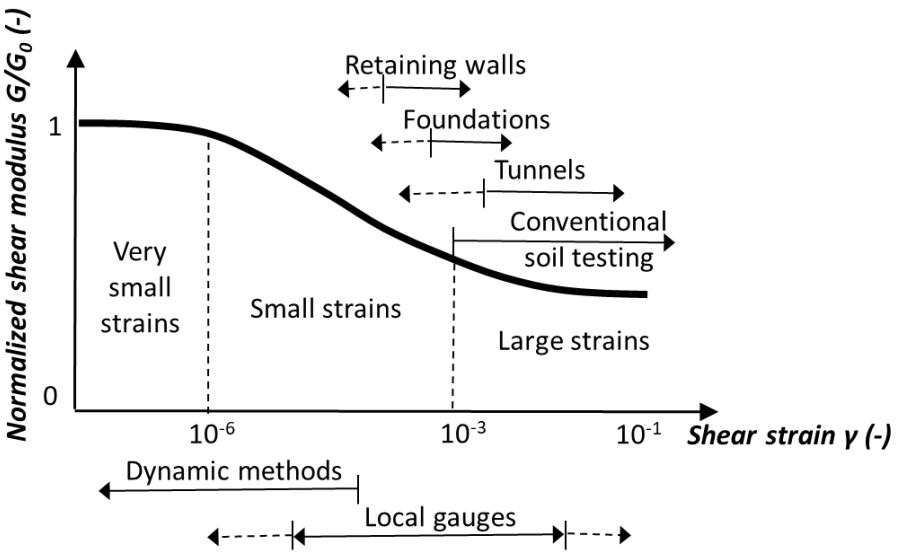

Fig. 1. Qualitative stiffness-strain decay curve of soils ([27,28] mod).

The transition between very small strain (defining almost elastic behaviour) and small strains is difficult to quantify and it can be generally assumed in the range $10^{-6} \leq \gamma \leq 10^{-5}$ [29]. The very small strain stiffness, or initial shear or Young's modulus, G_0 and E_0 respectively, corresponds to the maximum values of reduction curve; it is a fundamental property of all types of geotechnical materials including clays, silts, sands, gravels and rocks [29]. $\gamma \approx 10^{-3}$ is assumed as the transition value between small and large strains: it corresponds with the lower limit of classical laboratory testing (i.e. triaxial or oedometric tests with no special devices).

On the basis of empirical evidence [18, 30-34], the range of deformation induced by hydrocarbon activities can be assumed within the range of very small to small strains.

The small strain stiffness and its degradation behaviour depend mainly on the physical properties of the material as well as on the *in situ* condition. In particular, strain amplitude, void ratio, state of stress and over-consolidation ratio, plasticity index and the inter particle bonding like cementation have been highlighted as the most effective factors in the soil field [4,25, 35-37]. Fig. ***3*** shows the effects of some of the above-mentioned parameters on soil stiffness on the basis of empirical correlations[36].Even if the researches were focused on sands, the derived macro considerations are still valid, at least under a qualitative viewpoint, even for soft rocks hosting hydrocarbon reservoirs.

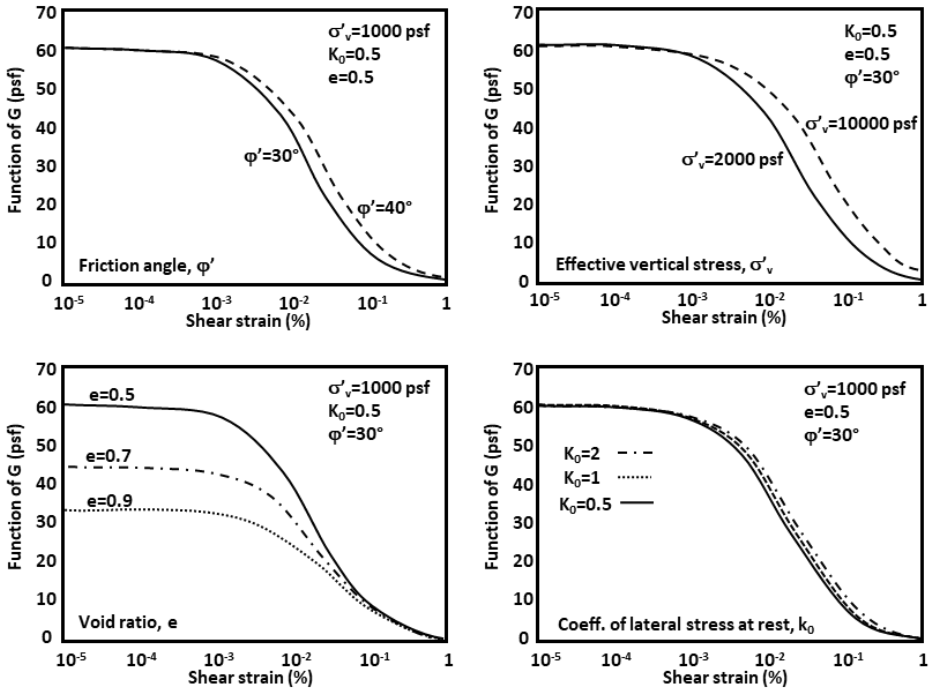

Fig. 2. Decay curve as a function of different parameters ([36], mod), where: effective vertical stress, σ'_v, is related to the dry matrix; void ratio, e, is the ration between void volume and solid volume; coefficient of lateral stress at rest, K_0, is the ration between initial effective minimum horizontal stress and initial effective vertical stress; and φ'is the drained friction angle.

Decay curves can be determined in the laboratory and or via *in situ* tests. Laboratory measurements are acquired via triaxial tests with strain measurements, benders elements (low voltage piezo-ceramic transducers for wave velocity measurements), resonant column and torsional shear [38,39]. *In situ* tests rely on seismic acquisition techniques that allow an indirect determination of the elastic stiffness in relation to wave propagation velocity measurement [38]. Each of these techniques has its own domain of investigation mainly on the basis of induced strain amplitude. In velocity measurements, the strain amplitude is typically 10^{-6}–10^{-7} so the relative techniques belong to the dynamic test class for the investigation of the very small strain stiffness. Static acquisition via conventional triaxial tests involves strain amplitude in the order of 10^{-2}–10^{-3} and they are conventionally used for the investigation of small strain stiffness; nevertheless, the adoption of local strain transducers allow for very small strain range investigation. Furthermore, torsional shear measurements are static or quasi-static tests and resonant column analysis provides satisfactory results in the very small strain range.

Although available, some of the above techniques are seldom used for routine investigation not only for their high costs but also because of the low level of measurement robustness. For example, test measurements on disturbed samples (due to the alteration of the original fluid content or the change in the acting stress state) may considerably vary from *in situ* test results. Bottom line, reliable experimental determination of very small strain stiffness and its degradation in relation to strain is not a trivial task. Moreover, empirical correlations as well as continuum small strain stiffness constitutive models have been developed over the last decades and they are available in the technical literature [38].Nevertheless, it should be noted that each empirical correlation must somehow always rely on experimental data, and that the scientific community has not fully agreed on a specific model.

3 Case study

The Po Plain-Adriatic Foredeep is an elongated foredeep basin lying parallel to the structural axes of the Northern Apennines. The infill consists of a thick succession of Messinian to Pleistocene sand-rich turbidite deposits [40]. Its geological setting is basically made up of alternating sand and clay layers (representing the Pliocene turbiditic sequence), generally with gas-bearing reservoirs overlaying the carbonate basin [19]. The typical lithological and stratigraphic sequence, extending down to 5 km depth, is shown in Fig. ***3***. Different reservoir configurations, in terms of depth, GOIP and shape factor, were set up so as to represent the Po Plain's hydrocarbon system.

The detailed description of the reference case, base case, represents the most probable configuration of a Po Plain gas reservoir. In others words, the reservoir is an axial symmetric anticline trap, located in a shaley sand lens (with no neighbouring aquifer) at about depth of 1500 meters. It is characterized by a thickness of 75 meters and a radius of 1.5 kilometres, giving a shape factor equal to 0.05. The gas originally in place equals 4.3 10^9 m^3_{sc} and the initial pressure is 159 bar. The hydraulic seal of the reservoir is ensured by a continuous clayey layer (the Santerno Formation) with an average thickness of 20 meters.

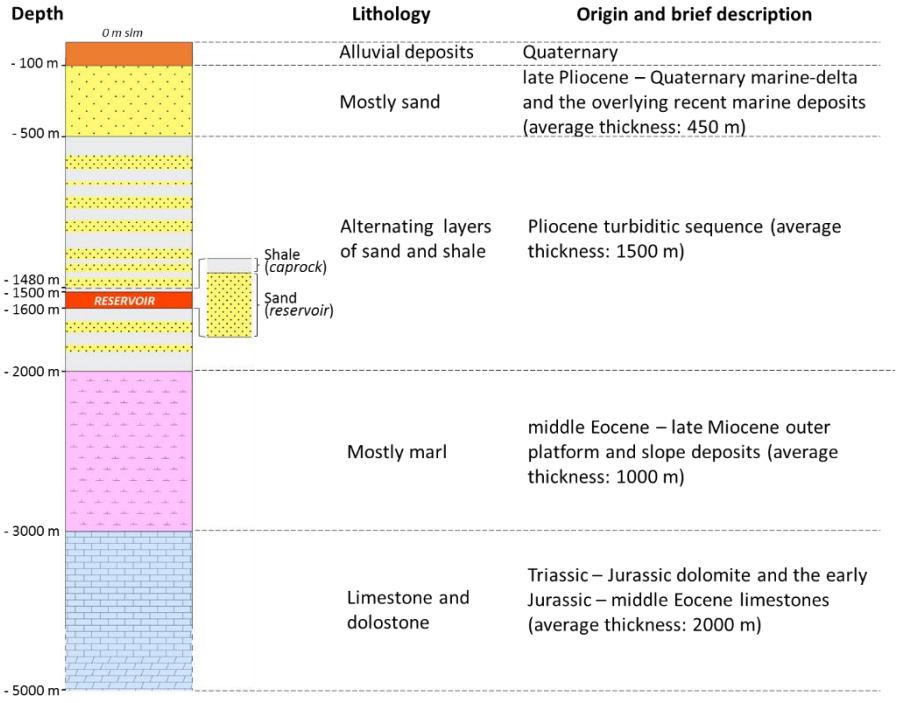

Fig. 3. Schematic stratigraphy (not to scale) of the geological sequence.

The evolution of subsidence potentially induced by gas production was evaluated with a numerical approach, via the definition and the characterization of three 3D models: static, dynamic and geomechanical [19, 30,31]. In particular, the static model at regional scale properly represents the main lithological, stratigraphic, geometrical and petrophysical features of the investigation domain, i.e. the Po Plain and the Adriatic Basin setting, as suggested by Benetatos et al. [19]. It was constructed adopting a simplified regional scale stratigraphy, considering homogeneous and continuous layers (Fig. ***4***). Based on preliminary sensitivity analyses, the extension of the model was deemed suitable for a correct description of subsidence evolution, ensuring that the imposed undisturbed boundary conditions (i.e. null normal displacement vector on the lateral boundaries) do not influence the solution of the rock mechanics simulation. Furthermore, the adopted tartan gridding technique provided good compromise between computational time and geological representativeness of the volume mainly involved by the phenomena under analysis.

The dynamic 3D finite difference method (FDM) model only represents the gas-bearing formation where the pressure changes (i.e. model forcing) with production strategy: a 10-year primary production phase from four wells was simulated until a recovery factor (the ratio between the cumulative gas production and the GOIP) of about 65% is reached [5]. Pressure

depletion in time (

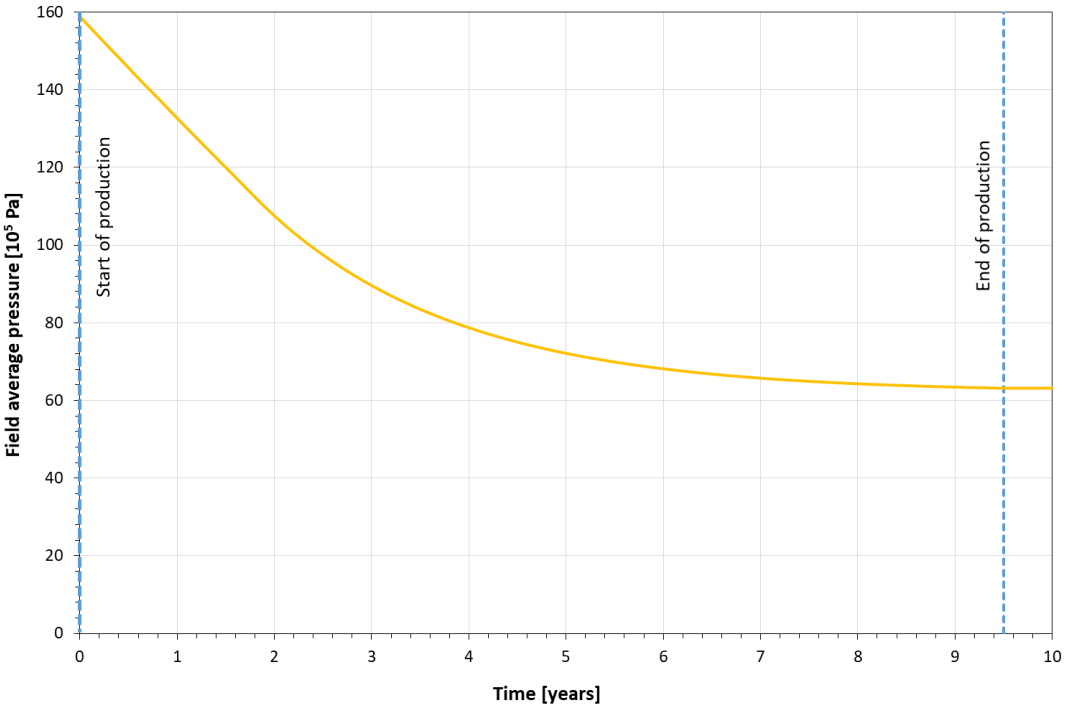

Fig. *5*) is typical of a depletion drive mechanism for gas reservoir, where hydrocarbon production relies on fluid expansion (i.e. the natural energy available in the reservoir). In this type of systems, most fluid production is commonly achieved in the early reservoir production life basically for economic purposes, with no consequence in terms of overall production efficiency [5]. Because the reservoir is a gas-bearing lent, the surrounding formations are characterized by a constant pore pressure equal to hydrostatic values during all reservoir production life.

Finally, on the basis of the static and dynamic models, a 3D finite element method (FEM) geomechanical model was set up and characterized via the definition of deformation and strength parameters (Table 1), as will be described later on. The mechanical analyses were performed adopting a poro-elastic perfectly plastic constitutive law and Mohr-Coulomb as strength criterion [4] together with the one-way coupling approach [41]. The model was initialized according to the normal hydrostatic pressure regime and gravity force (considering homogeneous and isotropic horizontal stress and a horizontal to vertical stress ratio equal to 0.8).

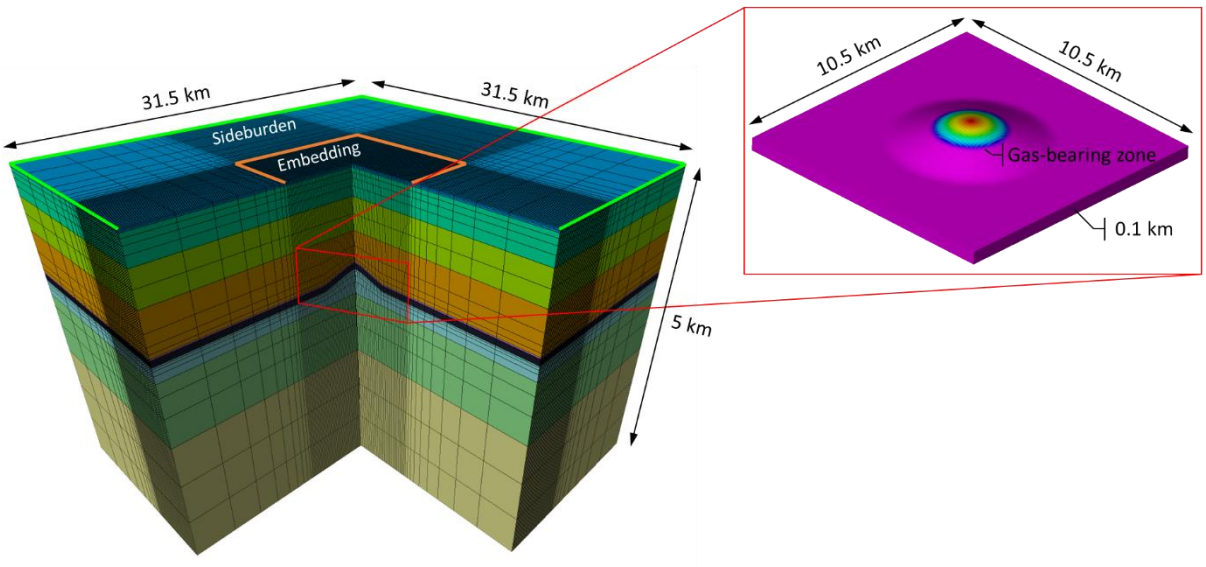

Fig. 4. Static model at regional scale and dynamic model (colours represent model zonation).

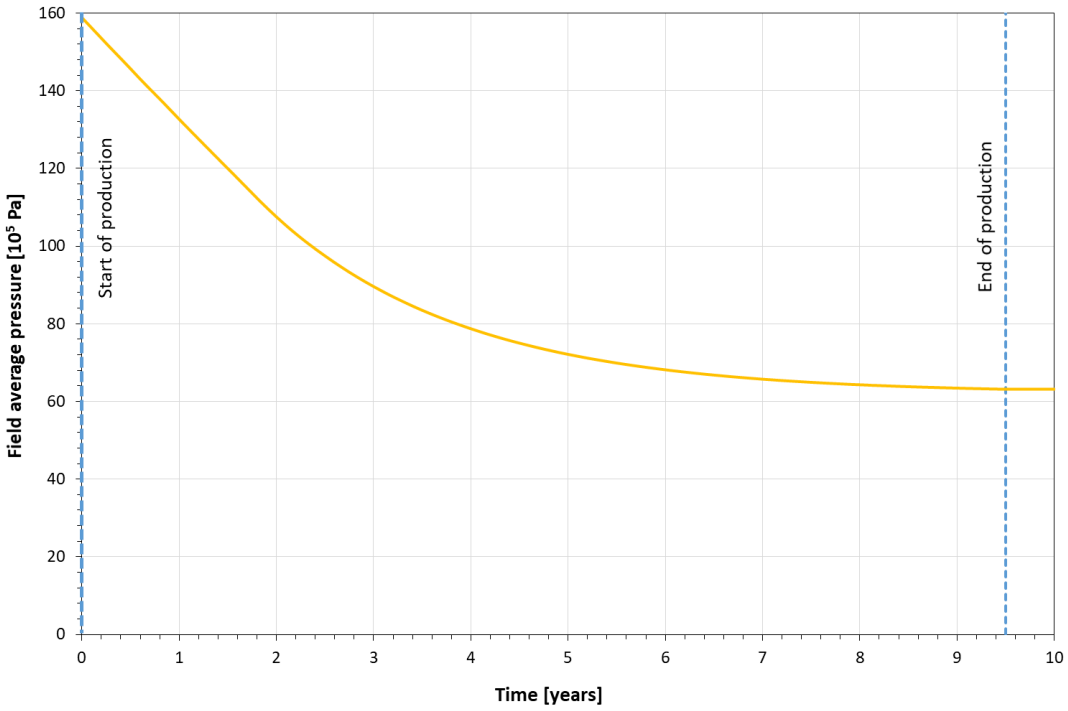

Fig. 5. Average static pressure evolution in time.

3.1 Determination of deformation input parameters

A coherent and complete dataset for rock characterization in terms of deformation and strength parameters was available from the data of two gas reservoirs located in the Po Plain. Triaxial lab tests on cap rock shale formations and reservoir shaley-sand formations where available together with sonic and density measurement at wellbore scale for each field. No lab test measurement was available for the definition of the decay curve; consequently, literature data was adopted, as described in the following.

3.1.1 Dynamic and static Young's moduli

Reservoir A [17] is located at an average depth of 1200 m TVD ssl; from a lithological standpoint, it is an alternation of sandstones and conglomerates, locally interbedded by marls or shaley limestones (the Sergnano Formation). The cap rock is represented by the overlying Argille del Santerno Formation. The available data consists of triaxial compression tests performed on the rock samples retrieved at well-A: after hydrostatic consolidation phases at confining pressures changing from 2 to 20 MPa, undrained compression tests were performed on the cap rock shale specimens and drained compression tests were executed on the reservoir sandstone specimens. Furthermore, sonic and density log measurements were acquired at the same well in a thousand meter interval, which corresponds to the Pliocene and the top of Lower Miocene (the Marne di Gallare Formation).

Reservoir B [18] is made up of alternating sands and silty sands, at an average depth of 1200 m TVD ssl. Triaxial compression tests were performed on cores retrieved at well-B both in the compact clays and in the dense sand under isotropically consolidated undrained conditions; the imposed confining stresses varied from (0.25–1) MPa and from (8–20) MPa. Additionally, sonic and density logs were acquired from cap rock (the Argille del Santerno Formation), the reservoir (the Porto Garibaldi Formation - Pliocene) and the under-burden formations at the same well.

The above mentioned data was analysed to identify the variation of static and dynamic moduli in relation to depth. Fig. ***6*** shows the static Young moduli as a function of depths equivalent to the lab confining stresses: values obtained only from the first load condition of triaxial laboratory tests were considered. In fact, during the loading condition phase

induced by primary production, the stress–strain path of a normal consolidated reservoir formation follows the critical state line (CSL) [17]. The dynamic values were obtained from the interpretation of sonic and density logs according to the relation between elastic waves velocity and mechanical properties of the formations under the hypotheses of linear isotropic elasticity [4]:

$$G = V_s^2 \rho$$

$$E = 2G(1 + v)$$

$$v = \frac{0.5\left(\frac{V_p}{V_s}\right)^2 - 1}{\left(\frac{V_p}{V_s}\right)^2 - 1}$$

where V_p is the P-wave velocity, V_s is the S-wave velocity, ρ is the total density of the formation, G is the shear modulus, E is the Young's modulus and v is the Poisson's ratio. The results are shown in Fig. *7*. The following general considerations can be highlighted:

1. in the investigated clastic sequences, made up of a silty to shaley sequence intercalated with arenaceous banks, the effect of lithology variation on the elastic modulus values can be considered negligible compared to the influence of depth. This behaviour was already pointed out by Ferronato et al. [42] and Teatini et al. [43]: they statistically analysed several *in situ* deformation measurements carried out in the offshore portion of the Po River basin by radioactive marker technique and they correlated the measurements adopting a power law;
2. the ratio between dynamic values from log interpretation and corresponding static values from triaxial tests is about 4 – 5.

In agreement with the above considerations, two power trend lines were defined to interpret the experimental data, and subsequently adopted for the geomechanical model characterization (Fig. ***6*** and Fig. *7*).

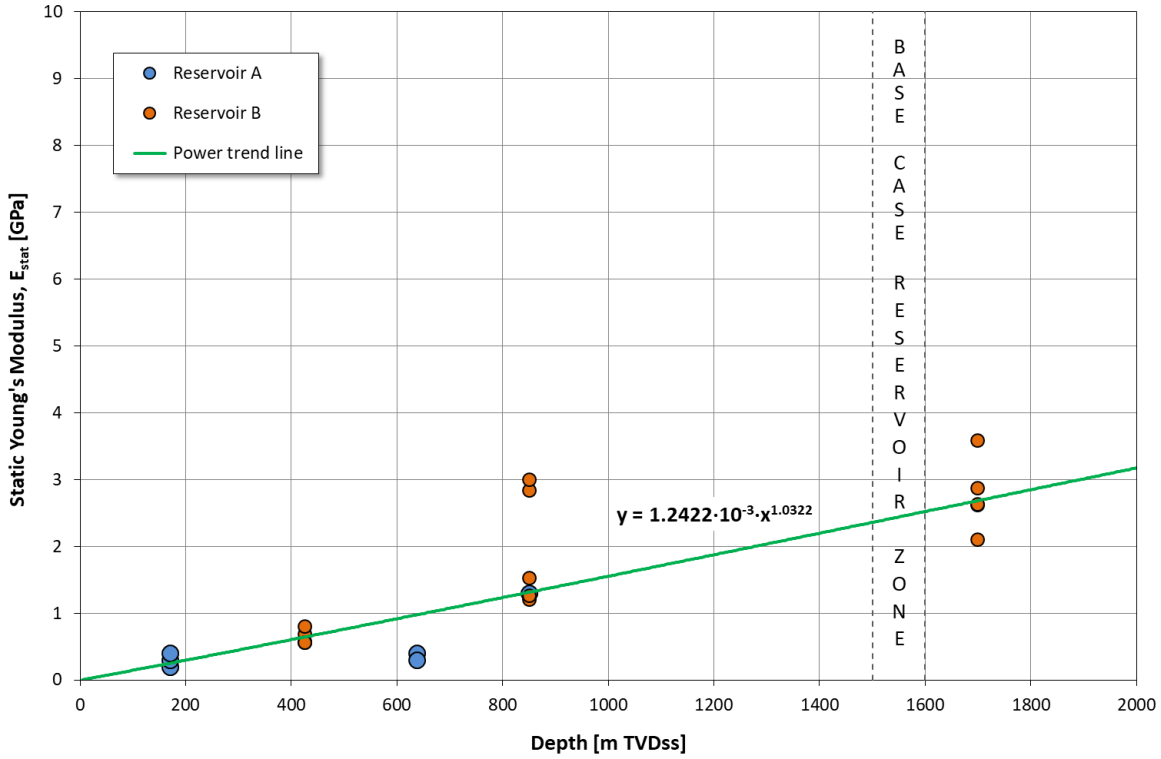

Fig. 6. Static Young's Modulus from lab analysis in relation to equivalent depth.

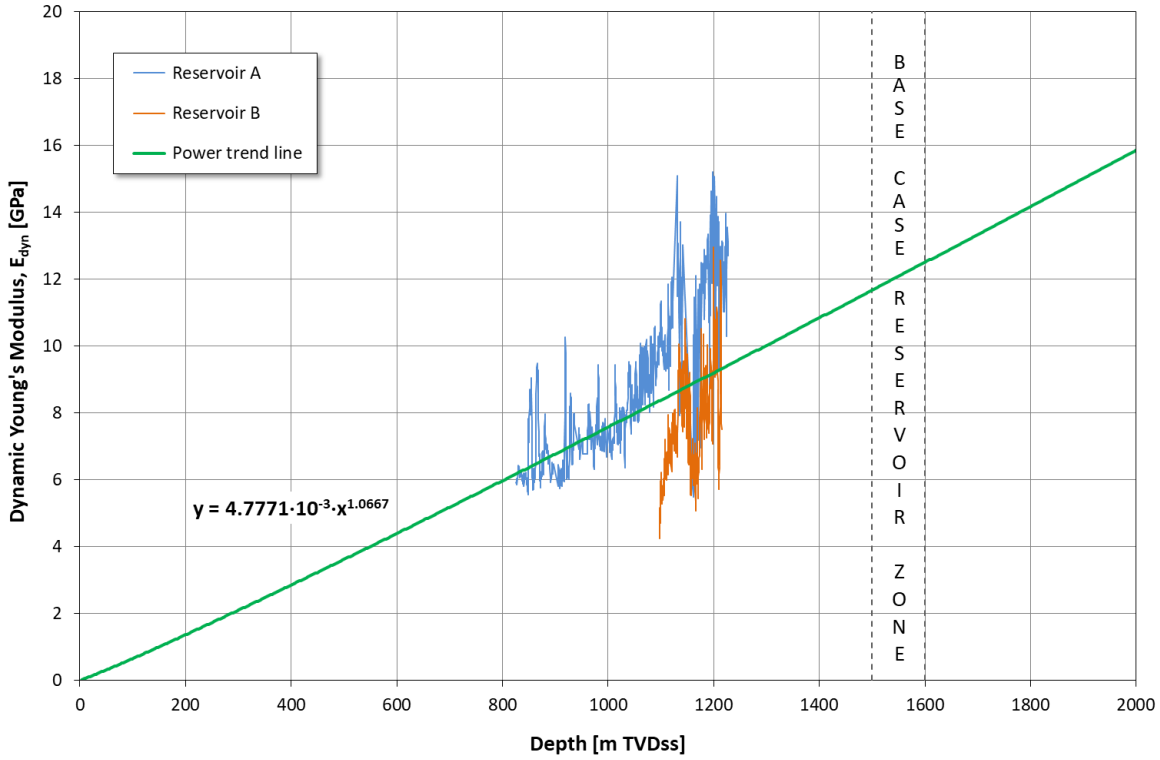

Fig. 7. Dynamic Young's Modulus from log data interpretation in relation to depth.

3.1.2 Decay curve

Fig. ***8*** shows the variation range of decay curves for normalized shear moduli, G/G_0 (where G_0 is the shear modulus at very small strain, or initial value), in relation to shear deformation, γ, considering different types of soil; it was obtained by collecting data from torsional tests related to geomaterials at shallow depths and from foundation engineering studies [44]. The normalized curve used for this research was obtained from Fig. ***8*** qualitatively, taking into account the shaley-sand lithology of the reservoir. Adopting the following relation [45]:

$$E_0 = G_0[2(1+\nu)]$$

$$\varepsilon_{axial} = \frac{\gamma}{1+\nu}$$

an equivalent curve expressed as normalized Young's modulus, E/E_0 (where E_0 is the Young's modulus at very small strain, or initial value), vs vertical strain, ε_{zz}, was defined. Subsequently, the equivalent normalized decay curve was rescaled (Fig. **9**a) to the ratio between the dynamic and static modulus values obtained from experimental data analysis of around 5 (see par. 3.1.1). Finally, the normalized and rescaled curve was multiplied by the dynamic Young's modulus value obtained from well log analysis at a depth of 1500 meters (i.e. the depth of the reservoir in the base case): the curve in Fig. **9**b is assumed as the real behaviour of the system. Thus, continuity was assigned to the mechanical response on the whole strain domain and therefore it is possible to recognize the evolution of the stiffness modulus according to the strain level reached during production.

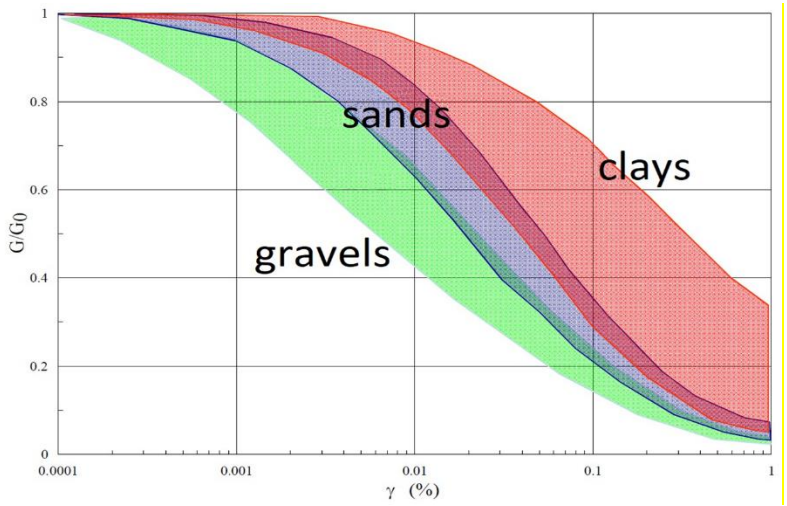

Fig. 8. Range of variation of normalized decay curves according to different soil typologies ([44], mod.).

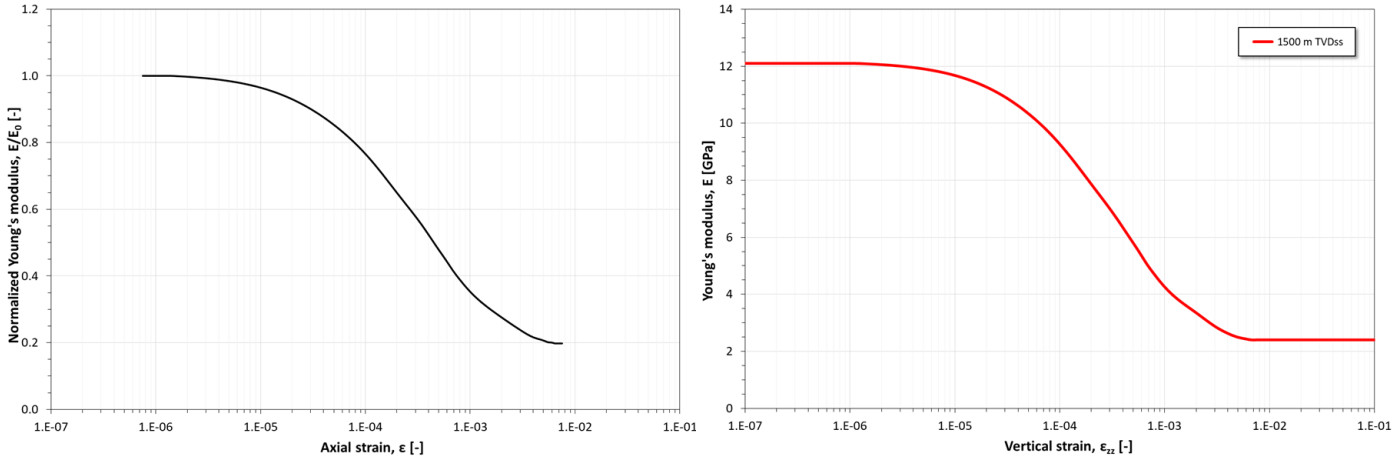

Fig. 9. (a) normalized and rescaled decay curve and (b) decay curve for 1500 meter depth reservoir.

4 Geomechanical model characterization

Based on depths and lithologies of the formations discretized in the geological model at regional scale (Fig. ***3***), 9 geomechanical classes (i.e. formations which exhibit constant, homogeneous and isotropic geomechanical behaviours) were identified and characterized according to the data analysis described in section 3.1 and integrated with data available in the technical literature [4]. Table 1 summarises the adopted values.

Table 1 Geomechanical classes for the base case, where**:** TVDss is the true vertical depth sub sea ν is the Poisson's ratio, c is the cohesion, ϕ is the friction angle.

Lithology	Class	Depth of top class	Thickness	Tot. Density	$\mathbf{E_{static}}$	$\mathbf{E_{dynamic}}$	ν	c	ϕ
	[-]	[m TVDss]	[m]	[kg/m^3]	[GPa]	[GPa]	[-]	[GPa]	[°]
Alluvial deposits	1	0	100	1900	0.2	0.2	0.39	0.2	38
Prevailing sands	2	100	400	2000	0.4	2.1	0.39	0.6	35
Sand-clay successions	3	500	500	2100	1.2	5.6	0.33	1.0	32
Sand-clay successions	4	1000	480	2200	1.9	9.5	0.33	1.0	32

Cap rock (Clay)	5	1480	20	2200	2.3	11.6	0.33	1.8	26
Reservoir (shaley sand)	6	1500	100	2300	2.4	12.1	0.33	0.9	34
Sand-clay successions	7	1600	400	2300	2.8	14.2	0.33	1.5	29
Marl	8	2000	1000	2400	40	40	0.3	2.0	35
Limestone and Dolostone	9	3000	2000	2600	50	50	0.3	4.0	45

5 Sensitivity analyses

Multi-variable sensitivity analyses were developed to generalize the results of the research, varying other key factors in subsidence evolution, mainly: reservoir depth, dimension (and GOIP) and shape factor [46,47]. For all simulated scenarios, the recovery factor and the normalized depletion, $\frac{\Delta p}{p_i}(\%)$:

$$\frac{\Delta p}{p_i}(\%) = \frac{(p_i - p_n)}{p_i}\%$$

where:

p_i is the initial fluid pressure of the reservoir, before production starts;

p_n is the static fluid pressure of the system at timestep n;

were kept constant to ensure consistency and comparability of the results obtained from different cases.

5.1 Description of analysed scenarios.

Three mechanical configurations were simulated:

I. overall geomechanical model is characterized by constant static elastic moduli (E_{stat});
II. overall geomechanical model is characterized by dynamic elastic moduli (E_{dyn});
III. reservoir formation, which is the volume affected by the largest strain variation, is characterized by the decay curve, instead the constant dynamic elastic moduli were input in the remaining portion of the model.

In the first two scenarios, the pseudo-elastic parameter values are defined as a function of depth according to the relation derived in section 3.1.1 from experimental data, but they do not vary according to the evolving formation deformation level induced by fluid pressure drop.

The three mechanical configurations aforementioned were simulated with discrete variation of the following reservoir parameters, where the range of variation was defined on the basis of Benetatos et al. [19]:

1) dimension: it varies from 0.2 to 5 times the dimension of the base case, thus GOIP value varies accordingly from 0.8 10^9 to 21.5 10^9 m^3_{SC} [5];

2) shape factor: it varies from 0.01 to 0.10, i.e. from disc to sphere; the corresponding results are not reported because they are identical to base case results;

3) depth (at the top of the reservoir): it varies from 300 to 2500 m TVDss. For each depth-dependent scenario, reservoir deformation and strength parameters were modified accordingly. In particular, for each depth-dependent scenario a dedicated decay curve was defined by multiplying the normalized and rescaled decay curve shown in Fig. **9**a by the dynamic Young's modulus value obtained from well log analysis at each reservoir depth.

Table 2 summarizes all the analysed cases, where case 3 (corresponding to the alpha numeric code V3_Z3) is the base case; Table 3 summarises the Young's modulus values adopted in the reservoir for each case, according to static, dynamic and decay curve scenarios.

The optimization of the timestep analysis was dictated by the decay curve scenarios to ensure an accurate representation of the evolution of the reservoir deformation response during production: a one-year time step was used for all simulated cases.

Table 2 Main characteristics of the sensitivity analysis scenarios, where: p_i is the initial reservoir pressure, Δp_{max} is the maximum pressure drop at the end of production, i.e. the difference between the initial reservoir pressure and the pressure at the end of production.

Sensitivity analysis parameter	Case	GOIP	Top Reservoir	Initial pressure	Induced Δp_{max}	Reservoir dimension	Alphanumeric Code
		[m^3_{sc}]	[m TVDss]	[10^5 Pa]	[10^5 Pa]		
GOIP (V)	1	0.8 10^9	1500	159	96	0.2V3	V1_Z3
	2	2.1 10^9				0.5 V3	V2_Z3
	3(*)	4.3 10^9				V3	V3_Z3
	4	10.5 10^9				2.5V3	V4_Z3
	5	21.5 10^9				5V3	V5_Z3
DEPTH (Z)	1	4.3 10^9	300	38	23	V3	V3_Z1
	2		800	88	52		V3_Z2
	3(*)		1500	159	96		V3_Z3
	4		2500	260	165		V3_Z4

(*)=base case

Table 3 Reservoir Young's modulus values for each case.

Alphanumeric Code	E_{static}	$E_{dynamic}$	E decay curve
	[GPa]	[GPa]	
V1_Z3	2.4	12.1	Decay curve @1500 m
V2_Z3			
V3_Z3 (*)			
V4_Z3			
V5_Z3			
V3_Z1	0.5	2.5	Decay curve@300 m
V3_Z2	1.3	6.4	Decay curve@800 m
V3_Z3 (*)	2.4	12.1	Decay curve@1500 m
V3_Z4	4.1	20.6	Decay curve@2500 m

(*)=base case

6 Results: base case

A detailed explanation of results from base case (V3_Z3) is given in the following paragraphs.

Fluid pressure drop due to hydrocarbon production induces increasing compaction of the reservoir formation, which propagates up to the surface generating an increasing subsidence cone until its maximum is reached in correspondence with the end of production life because no viscosity effects are present.

Induced vertical deformation of the reservoir during production varies from 10^{-4} to 10^{-3}, which with a progressive decay of the stiffness properties. Instead, the horizontal deformation is negligible during all reservoir production life ($<10^{-6}$). Fig. ***10*** shows the monotonic reduction of reservoir Young's modulus as a function of the induced vertical strain from the initial dynamic value tending to the static value at the end of production. The same results can also be shown as temporal and spatial evolution of the Young's modulus in the reservoir (Fig. ***11***): its homogeneous distribution derived from the simplified assumption in the model construction and characterization (axial-symmetry structure, homogeneous distribution of all parameters with consequence homogenous spatial evolution of pressure).

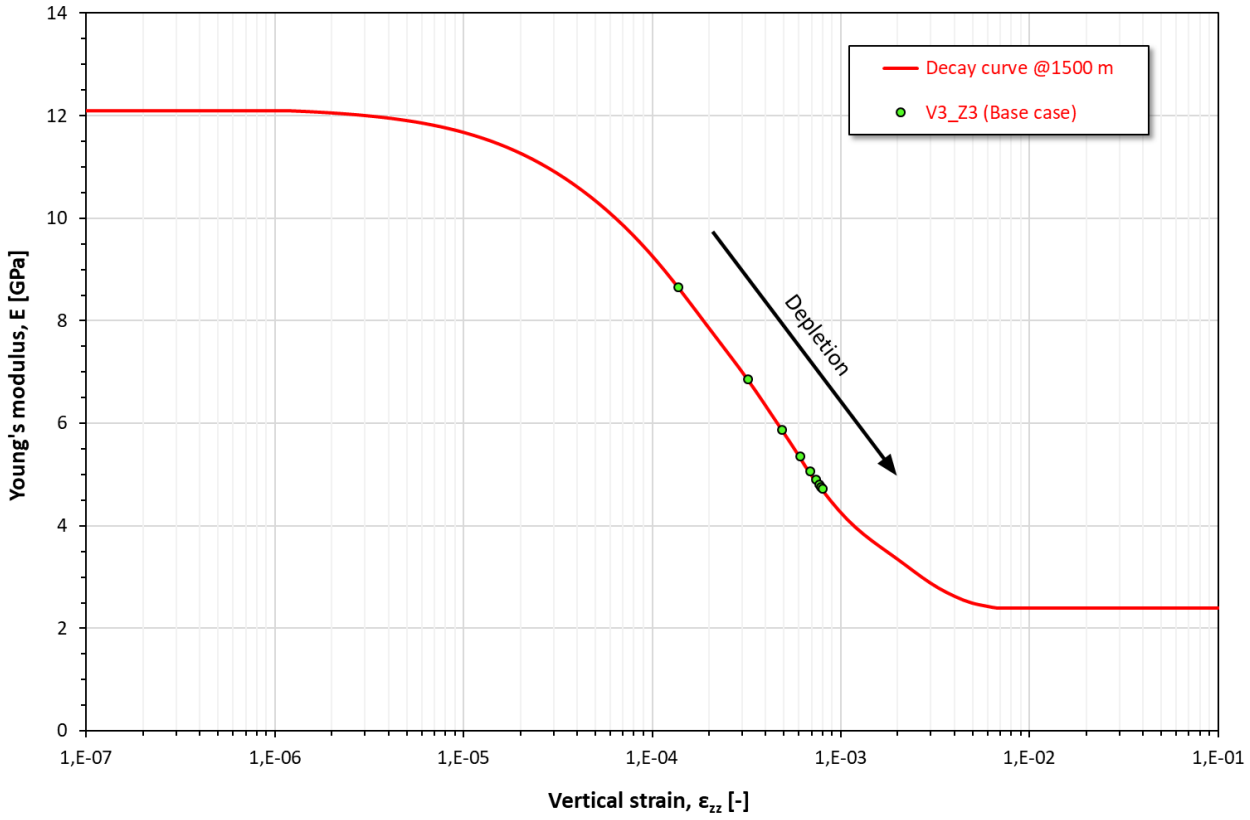

Fig. 10. Base case with decay curve (case code: V3_Z3, E_{decay}): variation of the reservoir Young's modulus as a function of the vertical strain. Dots represent the simulation results for each time step.

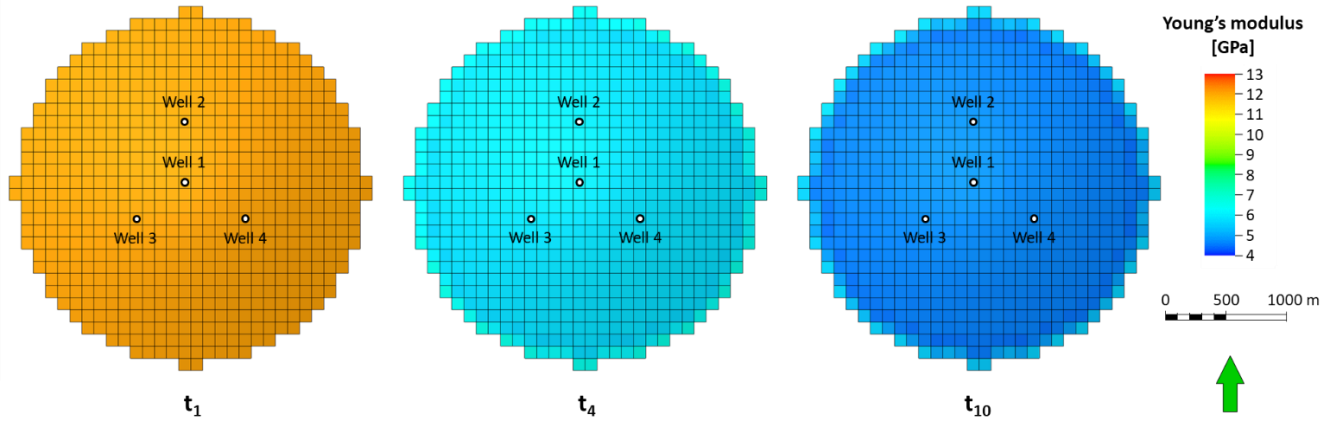

Fig. 11. Base case with decay curve (case code: V3_Z3, E_{decay}): Young's modulus distribution at the top of the reservoir at different timesteps (t_1= one year of production, t_4= four years of production and t_{10}= end of production).

As for induced subsidence, Fig. ***12*** shows the temporal evolution of the maximum vertical displacement at surface (at well 1) according to static, dynamic, and decay curve configurations, for each timestep; whereas Fig. ***13*** shows the corresponding areal extension of the induced subsidence at the end of production (t_{10}) considering a threshold of vertical displacement equal to 1 millimeter. Even if this threshold has no engineering meaning, it was set for the purpose of the work. The results clearly show the assumption of constant dynamic values better approximate, in an optimistic manner, the result obtained under the assumption of the decay curve.

The base case shows an important element: even if the mechanical stiffness of the reservoir evolves towards the static modulus value during production, the relative induced subsidence both in terms of vertical displacements and areal extension can be approximated with higher accuracy by the constant dynamic modulus assumption.

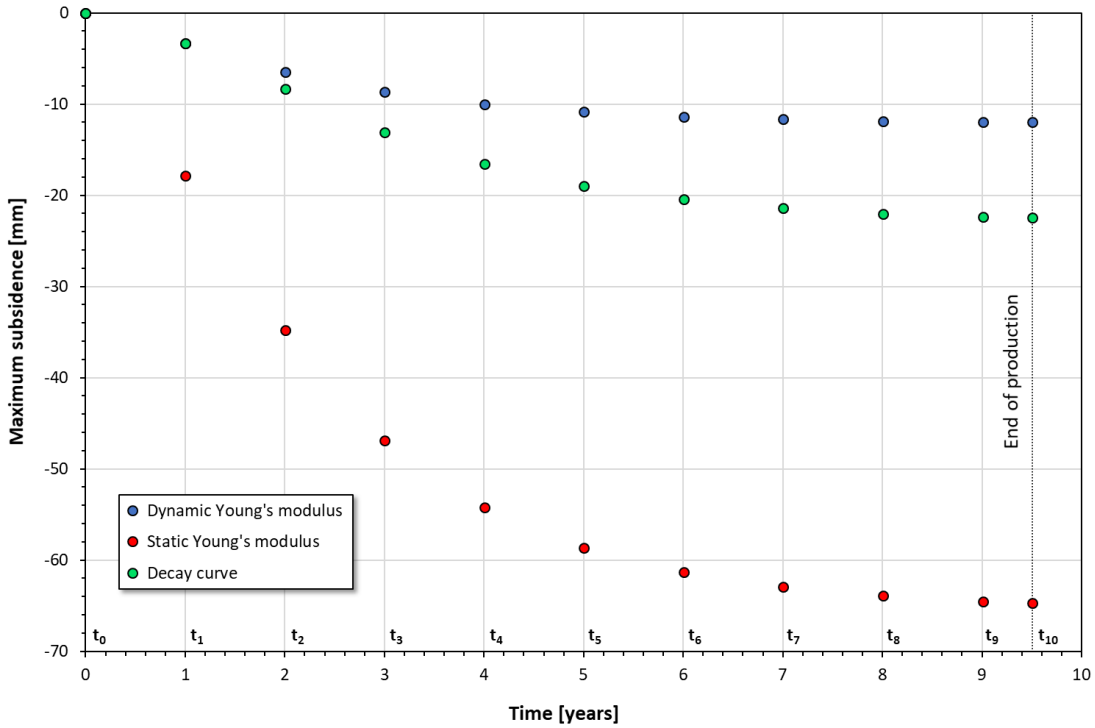

Fig. 12. Base case: maximum subsidence at each timestep as a function of the assigned Young's modulus.

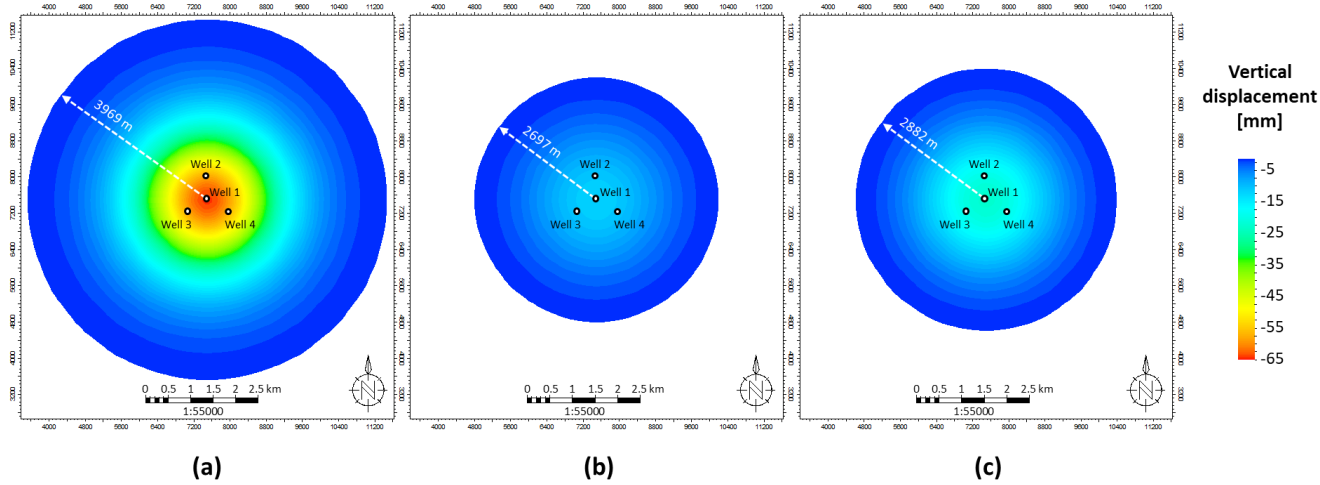

Fig. 13. Base case: surface extension of the subsidence cone at the end of production (t_{10}) in case of (a) static Young's modulus, (b) dynamic Young's modulus and (c) decay curve.

7 Results: sensitivity analysis

The base case behaviour was confirmed by the results gathered from sensitivity analyses on multi-variable scenarios, which also allow the identification of confidence ranges in approximating the results of the decay curve assumption. Regarding all analysed configurations and during the entire production history, the evolution of the state of stress both outside and especially inside the reservoir lies widely within the elastic domain.

For each GOIP case and reservoir depth configuration, the vertical deformation induced in the reservoir during production evolves always in the range ($10^{-4} \div 10^{-3}$) with a progressive decay of Young's modulus from dynamic to static values. Fig. ***14*** shows the monotonic reduction of the reservoir Young's modulus as a function of the induced vertical strain considering different reservoir GOIPs at 1500 meter depth (base case depth). Whereas, assuming a constant GOIP equal to the GOIP of the base case, Fig. ***15*** shows the reduction of the Young's modulus for different reservoir depth configurations on the corresponding decay curve.

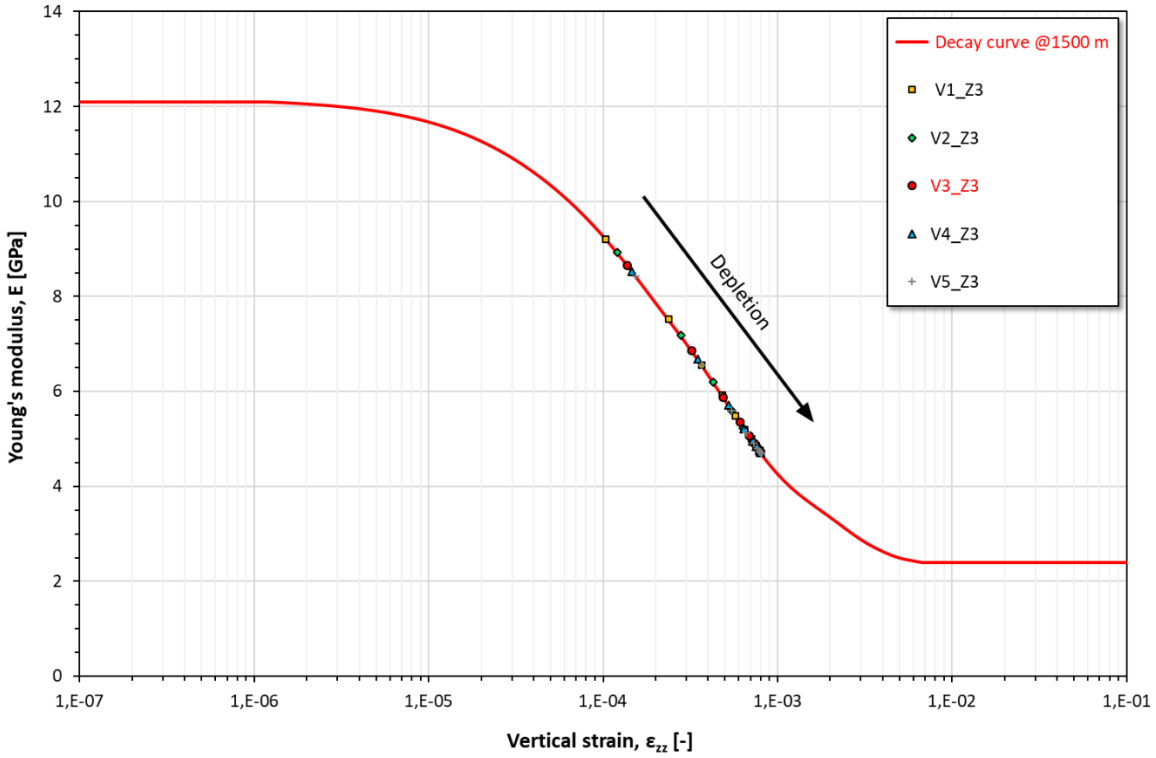

Fig. 14. Sensitivity analysis concerning different GOIPs: variation of the reservoir Young's modulus as a function of the vertical strain inside the reservoir.

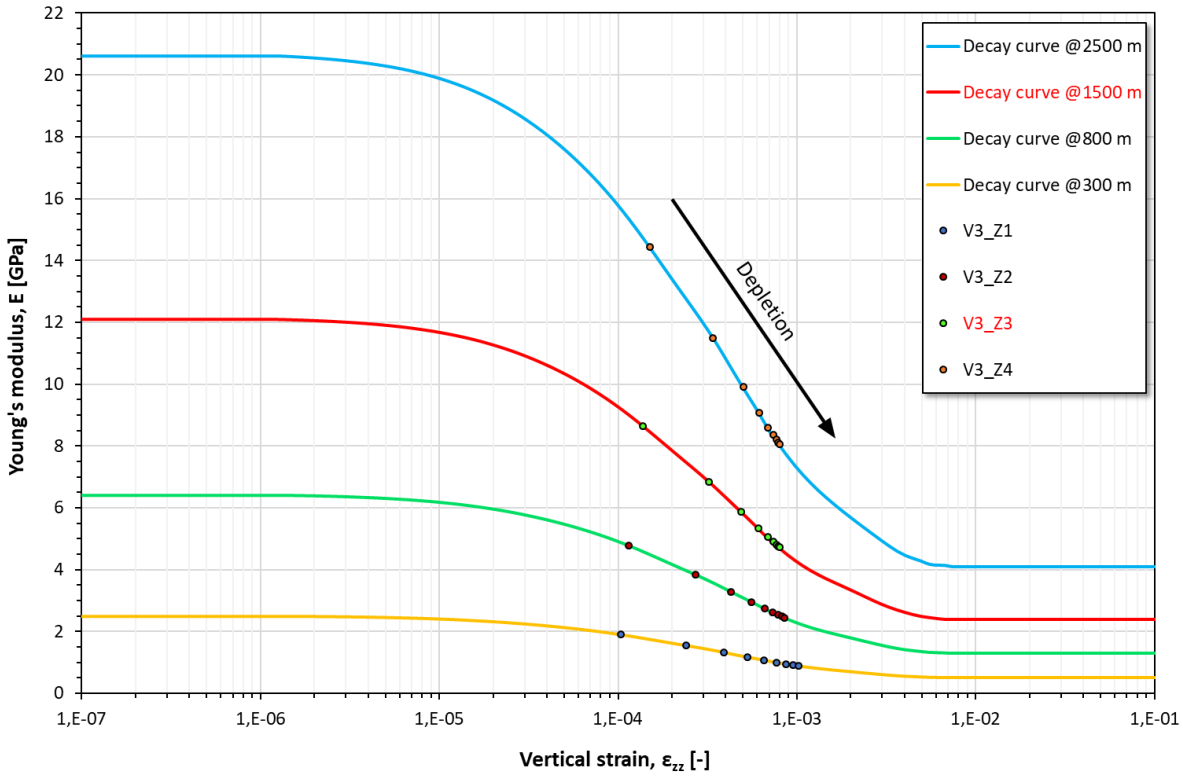

Fig. 15. Sensitivity analysis concerning different depths: variation of the reservoir Young's modulus as a function of the vertical strain inside the reservoir.

For each scenario (Table 2), the evolution of the subsidence phenomena was simulated according to static, dynamic and decay curve configurations and the results were compared in terms of relative error (%) among the constant (static or dynamic) deformation parameter assumption and the corresponding decay curve scenarios:

$$Error\ on\ maxium\ subsidence = \frac{\left(z_{cost}^{max} - z_{decay}^{max}\right)}{z_{decay}^{max}}\%$$

where:

z_{cost}^{max} is the maximum vertical displacement under the hypothesis of constant (static or dynamic) deformation parameters at each timestep;

z_{decay}^{max} is the maximum vertical displacement under the hypothesis of decay curve at each timestep.

Fig. ***16*** shows the evolution of the relative errors related to the maximum subsidence value for each timestep as a function of normalized depletion, $\frac{\Delta p}{p_i}(\%)$, for all the simulated cases; while Fig. ***18*** represents the variation of the relative errors referred to the radius of the induced subsidence cone at surface as a function of normalized depletion, $\frac{\Delta p}{p_i}(\%)$, for all the simulated cases.

The following general observations can be made:

1) for all scenarios, the static elastic parameter assumption always corresponds to the higher error values with the wider confidence interval, both in terms of maximum vertical displacement and cone radius;
2) for each case, the relative errors show a monotonic reduction in relation to normalized depletion increase;
3) the relative errors related to the subsidence radius are significantly smaller than those concerning the maximum subsidence.

Concerning relative errors due to <u>static</u> parameter assumption, the following distinctive features can be recognized:

1) it always represents a conservative approach in subsidence analysis, in terms of both maximum vertical displacement and cone radius;
2) the relative error is maximum during the early production stage characterized by very small rock deformation value (induced by limited pressure drop) and consequent stiffer material behaviour; as induced strain level increases, static assumption better approximates the real system behaviour;
3) at each timestep, the relative error related to maximum vertical displacement is slightly affected by GOIP variation;
4) instead, reservoir depth strongly affects the relative error values: deep compact reservoirs obviously show a stiffer deformation behaviour, whereas lower values of elastic parameters better describe the shallow reservoir deformation behaviour;
5) the error related to the maximum vertical displacement varies from +150% to +500% with confidence interval of Figure 17; the error related to the cone radius varies from +20% to +130% with confidence interval of Figure 19;

Concerning relative errors due to <u>dynamic</u> parameter assumption, the following distinctive features can be discerned:

1) it always represents an optimistic approach in subsidence analysis, in terms of both maximum vertical displacement and cone radius;
2) the relative error is negligible at the early production stage while it grows monotonic according to increasing pressure drop end consequent induced strain level;
3) the error related to the maximum vertical displacement varies from 0% to -50% with confidence interval of Figure 17; the error related to the cone radius varies from 0% to -15% with confidence interval of Figure 19.

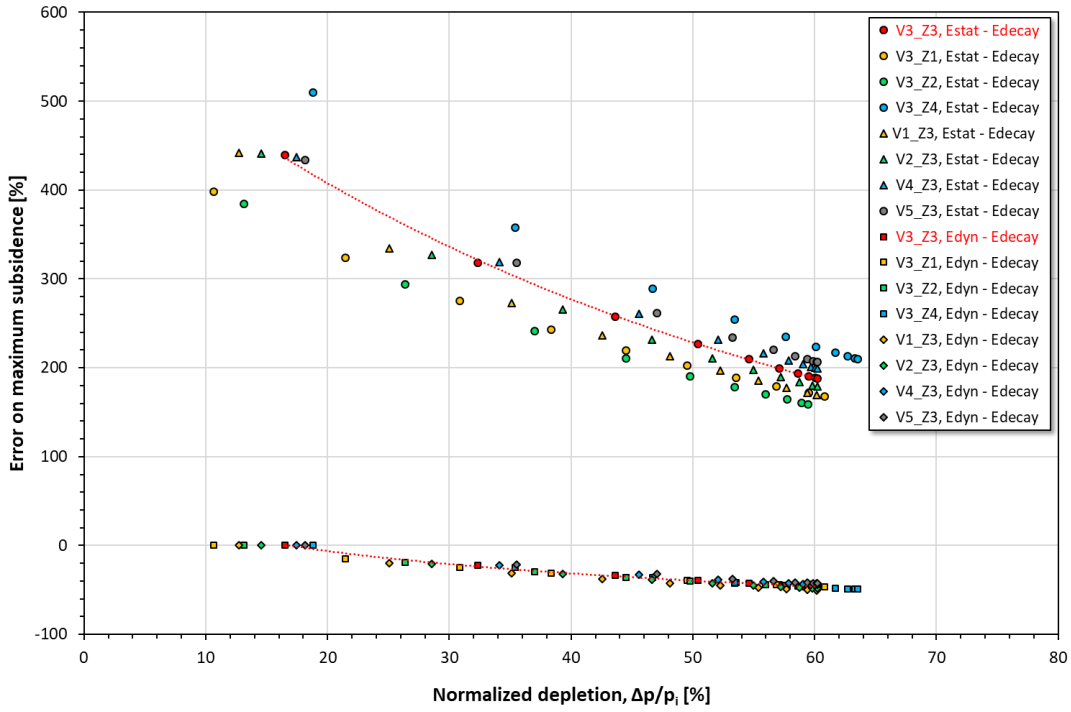

Fig. 16. Relative error (%) of the maximum vertical displacement in relation to the normalized pressure drop, $\frac{\Delta p}{p_i}(\%)$, for all the simulated cases. In red the base case scenarios.

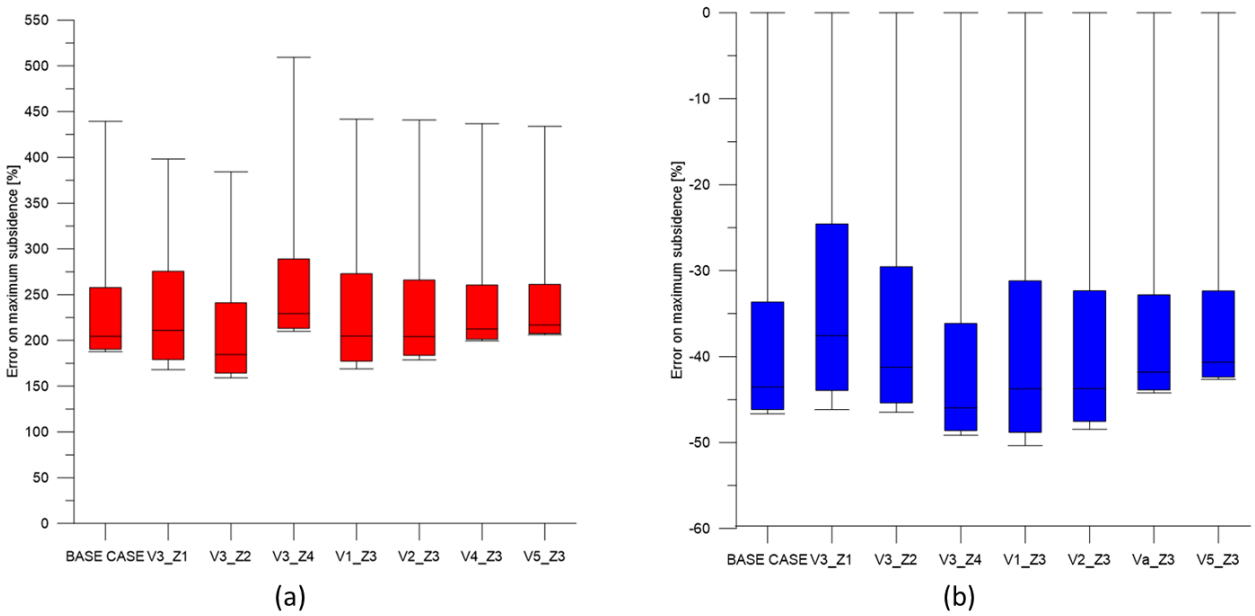

Fig. 17. Relative error (%) of the maximum vertical displacement for (a) static and (b) dynamic scenarios.

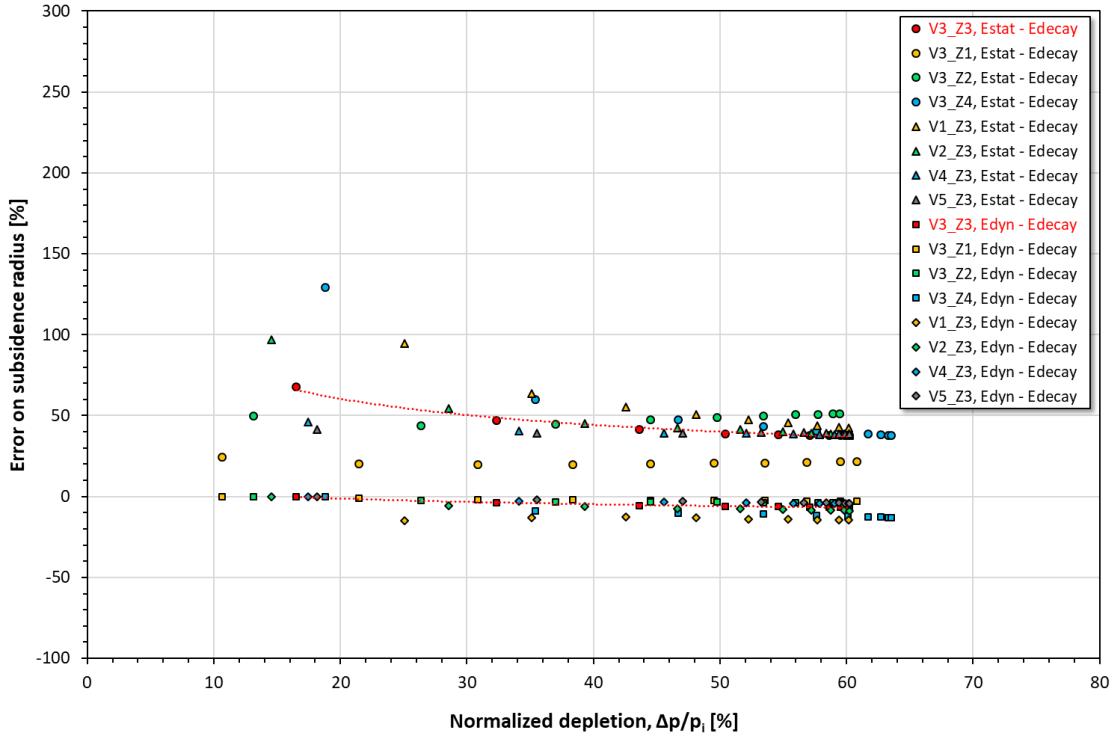

Fig. 18. Relative error (%) of the subsidence radius in relation to the normalized pressure drop, $\frac{\Delta p}{p_i}(\%)$, for all the simulated cases. In red the base case scenarios.

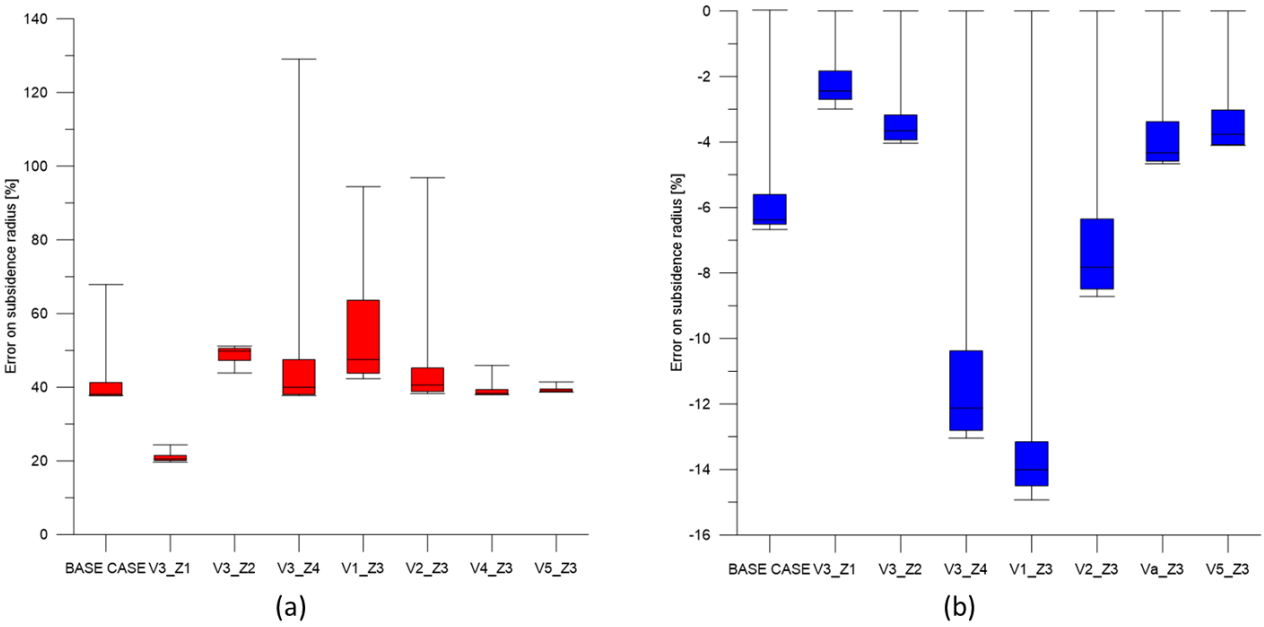

Fig. 19. Relative error (%) of the subsidence radius for (a) static and (b) dynamic scenarios.

8 Real case study

The distinctive features highlighted by the sensitivity analysis on synthetic models were validated via the analysis of a real gas-bearing formation, Reservoir A. As pointed out in section 3.1.1, the pseudo-elastic parameters of the reservoir formation showed a ratio of 4 – 5 between dynamic values from log interpretation and corresponding static values from triaxial tests.

For sake of brevity, only the main features of the case study are recalled, for a detailed description please consider Coti et al. [17]. The case study refers to an underground gas storage (UGS) operated in a depleted reservoir in Northern Italy. UGS basically consists of injecting gas during the summer season and producing it during the winter months and it is a widespread practice which serves to meet today's growing energy demand as well as daily and seasonal oscillation demands [34]. Three 3D numerical models were available for Reservoir A: a static geological model at regional scale; a multiphase flow numerical model of the reservoir which provide the forcing function applied to the geomechanical (i.e. the historical pore pressure evolution in time and space due to production/injection operations) and a geomechanical model populated with the available deformation and strength parameters. Measurements of time and space evolution of the reservoir fluid pressure and of the induced land surface movements were collected for over more than ten years of seasonal production/injection cycles. In particular, the occurrence, pattern and magnitude of land displacement above the field was provided by analysis of satellite images (PSInSARTM). Based on synthetic aperture radar (SAR) data acquired over the same area at different times, the PSInSARTM methodology provides millimetric-scale movements of large zones [34,48,49]. Monitoring of land movements coincided with storage activities and no data were available during primary production. As a consequence, data acquired during a production cycle (from November to April) was analysed: the induced pressure drop at the end of production (around 40 10^5 Pa) was enough to induce measurable ground subsidence (Figure 20). Figure 20 shows the comparison between subsidence data measured in three points (P1, P2, P3) above the reservoir and the simulated vertical displacement according to static deformation parameter and dynamic deformation parameters. Figure 21 represents the variation of the relative errors referred to the surface vertical displacement as a function of time. A part for the scattering intrinsic in real measurements, the results of the case study are in line with the results of the sensitivity analysis: the static scenarios represents a strong conservative assumption and the discrepancy between simulated and measured vertical displacements increases with production (i.e. with pressure drop increment); whereas the dynamic scenarios is an optimistic approach with an acceptable error in the system simulation which decreases with production.

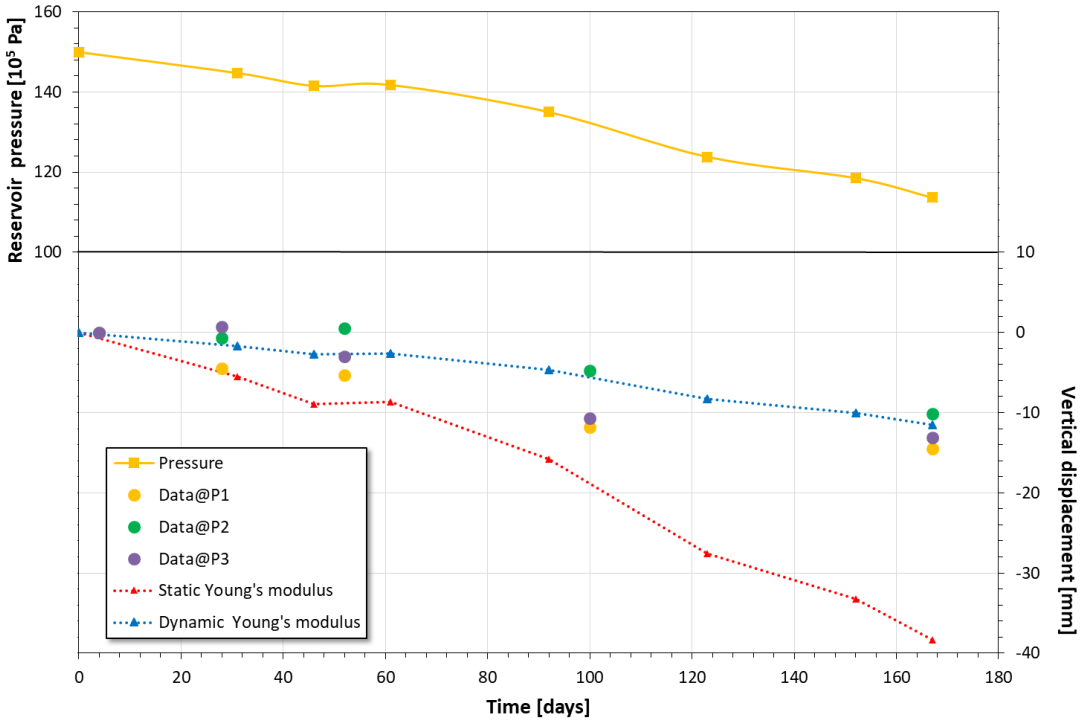

Fig. 20. Reservoir pressure variation in relation to time; measured and simulated vertical displacements in relation to time.

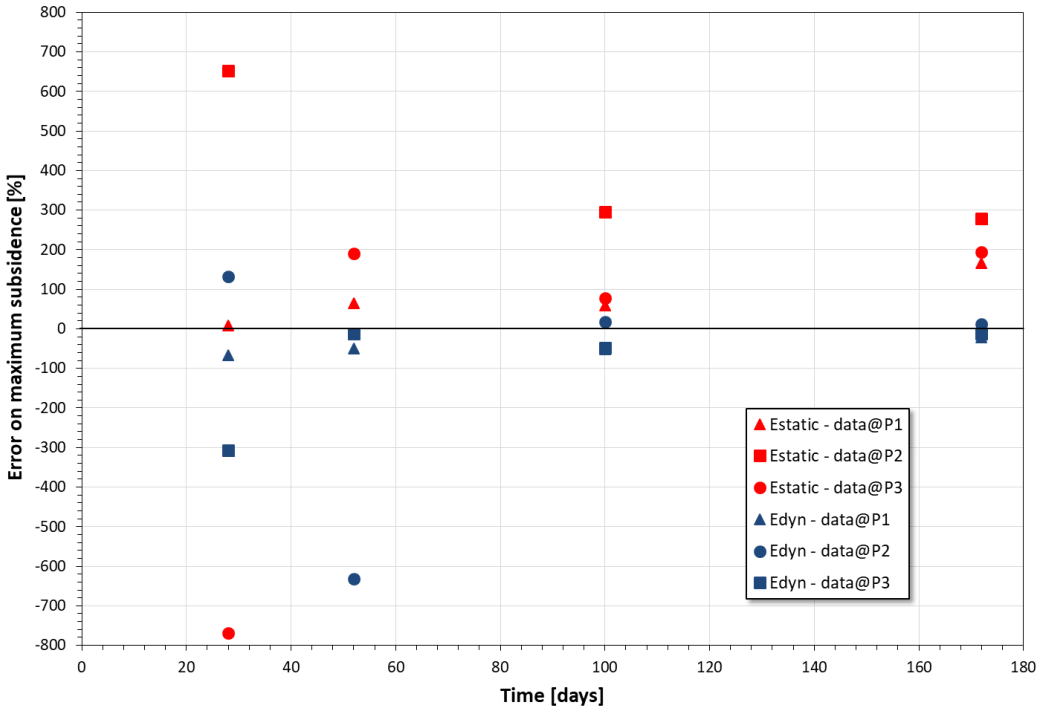

Fig. 21. Relative error (%) of the maximum vertical displacement in relation to time, for static and dynamic scenarios.

9 Conclusion

The scope of the research is to cast some light on the reliability level of the prediction of the subsidence phenomena induced by hydrocarbon production from shallow medium depth clastic formations, which contain most of the reserves in the largest known reservoirs and could exhibit an important non-linear influence of strain on formation stiffness. A series of multi-variable sensitivity analyses were developed to quantify the discrepancy in subsidence forecast deriving from the assumption of constant (static or dynamic) pseudo-elastic parameters values along all reservoir production life instead of inputting into the model a decay curve. The case studies, even synthetic, are a compound of standard features representing gas-production from a clastic reservoir (in terms of thermodynamic, petrophysical, geological and geomechanical characteristics/behaviour as well as production profile) so as to analyse the response of a macro category.

The results of all the analysed cases (which differ in relation to reservoir depth, dimension and relative GOIP, and shape factor) clearly show that even if the mechanical response of the reservoirs evolves towards the static modulus value during production, the relative induced subsidence both in terms of vertical displacements and areal extension, is approximated with higher accuracy by the constant dynamic modulus assumption during all reservoir production life. In fact, subsidence phenomena can be explained by the superposition principle: early in production life, the reservoir formation is stiffer and it reacts to pressure drop with small deformation according to dynamic pseudo-elastic value; due to progressive degradation, the formation stiffness tends to the static value, at the end of production life if at all. Hence, the largest pressure drop affected the reservoir formations in their original maximum stiffness condition or slightly degraded.

The distinctive features highlighted by the sensitivity analysis on synthetic models were validated via the analysis of Reservoir B. The real case study features as in line with the assumptions of the synthetic scenarios: a gas bearing formation made up of alternating sands and silty sands, at an average depth of 1200 m TVD ssl, characterized by a substantial discrepancy between dynamic values from log interpretation and static values from triaxial tests.

Based on the obtained results, the adoption of constant dynamic parameters value turns out to be the most reliable solution in case of medium depth clastic reservoir: even if the subsidence forecast is underestimated, the relative error is always acceptable if compared to relative error obtained from the case of constant static parameter scenarios. Furthermore, dynamic values better approximated formation behaviour at the early reservoir production stage, with negligible errors in subsidence prediction, when the level of uncertainty in all reservoir features and in the phenomenological evolution related to production exploitation is the highest. Later on, reservoir behaviour in terms of pore pressure evolution and induced subsidence can be monitored and the data used to calibrate the provisional models so as to gather more accurate subsidence prevision.

An interesting future development of the research can be the comparison with results from a representative number of real case studies to assess the effects of reservoir features such as heterogeneity, anisotropy, geometrical and structural peculiarities and aquifer connection ad support. The drawback is finding coherent and complete public datasets with not only the monitored subsidence measurements but also reservoir geometrical, geological geomechanical features together with the production history.

References:

1. Bau´, D., Gambolati, G., Teatini, P. (2000). Residual land subsidence near abandoned gas fields raises concern over northern Adriatic coastland. EOS, Trans. Am. Geophys. Union 81, No. 22, 245–249.
2. Bau´, D., Ferronato M., Gambolati, G., Teatini, P. (2002). Basin-scale compressibility of the northern Adriatic by the radioactive marker technique. Geotechnique 52, No. 8, 605–616
3. Rocca V. (2009). Development of a fully coupled approach for evaluation of wellbore stability in hydrocarbon reservoirs. American Journal of Environmental Sciences vol. 5, issue 6, 2009, pp 781-790, ISSN: 1553345X. DOI: 10.3844/ajessp.2009.781.790
4. Fjær, E., Holt, R.M., Horsrud, P., Raaen, A.M., Risnes, R. (2008). Petroleum related rock mechanics. Development in Petroleum Science (2nd Edition), vol. 53. Elsevier Science Publishers B.V, Amsterdam.
5. Dake L.P. (1998). Developments in Petroleum Science, 8. Fundamentals of reservoir engineering. ISBN 0-444-41830-X, 1978 ELSEVIER SCIENCE B.V. A
6. Lancellotta R. (2012). Geotecnica. Zanichelli ed.
7. Beccari M., Romano U. (2005). Encyclopaedia of hydrocarbons. Istituto della enciclopedia italiana fondata da Giovanni Treccani S.p.A.
8. Aminzadeh F., Dasgupta S. N. (2013). Developments in Petroleum Science. Volume 60, 2013, Elsevier,https://doi.org/10.1016/B978-0-444-50662-7.00002-0
9. Dean R. H., Gai X., Stone C. M., Minkoff S. E. (2003). A comparison of techniques for coupling porous flow and geomechanics. Paper SPE 79709 presented at the SPE Reservoir Simulation Symposium, Houston, Texas, U.S.A., 3-5 Feb. 2003.
10. Samier P., Fontaine G. (2003). Coupled analysis of geomechanics and fluid flow in reservoir simulation. Paper SPE 79698 presented at the SPE Reservoir Simulation Symposium, Houston, Texas, U.S.A., 3-5 Feb. 2003.
11. Settari A., Maurits F.M. (1995). A coupled reservoir and geomecanichal simulation system. Paper SPE 50939 (September 1998), presented at the 1995 SPE Reservoir Simulation Symposium, San Antonio, Texas, U.S.A., 12-15 Feb. 1995.
12. Settari A., Walters D. A. (1999). Advances in couplet geomechanical and reservoir modeling with applications to reservoir compaction. Paper SPE 51927 presented at the SPE Reservoir Simulation Symposium, Houston, Texas, U.S.A., 14-17 Feb. 1999.
13. Tran D., Settari A., Nghiem L. (2002). New iterative coupling between a reservoir simulator and a geomechanics module. Paper SPE 78192 presented at the SPE/ISRM Rock Mechanics Conference, Irving, Texas, U.S.A., 20-23 Oct. 2002.
14. Rocca V. (2008). Approaches to geomechanical modelling in reservoir engineering. GEAM
15. Rutqvist J., Vasco D. W., Myer L. (2010). Coupled reservoir-geomechanical analysis of CO2 injection and ground deformations at In Salah, Algeria. International Journal of Greenhouse Gas Control (Elsevier). Volume 4, Issue 2, March 2010, Pages 225-230, https://doi.org/10.1016/j.ijggc.2009.10.017
16. Rutqvist J., Birkholzer J., Tsang C. (2006). Modeling of geomechanical processes during injection in a multilayered reservoir – caprock system and implications on site characterization. Proceedings, CO2SC. Symposium 2006 Lawrence Berkeley National Laboratory, Berkeley, California, March 20-22, 200
17. Coti C., Rocca V., Sacchi Q. (2018). Pseudo-Elastic Response of Gas Bearing Clastic Formations: An Italian Case Study. Energies 2018, 11, 2488; DOI:10.3390/en11092488
18. Codegone, G., Rocca, V., Verga, F., Coti, C. (2016). Subsidence modeling validation through back analysis for an Italian gas storage field. Geotechnical and Geological Engineering, vol. 34 (6), pp. 1749-1763. ISSN 0960-3182.
19. Benetatos C., Codegone G, Deangeli C., Giani G. Gotta A., Marzano F., Rocca V., Verga F. (2017) Guidelines for the study of subsidence triggered by hydrocarbon production GEAM - Geoingegneria Ambientale e Mineraria, Anno LIV, n. 3, dicembre 2017, 85-96, ISSN: 11219041
20. Burlan J.B. (1979) Contribution to discussion on session 4. In Proc. 7th Eur. Cnf. Soil Mech. vol. 4, pp 137, Brighton. SMFE

21. Cole K.W. and Burland J.B. (1972). Observation of retaining wall movements associated with a large excavation. In Proc. 5t ECSMFE, vol. 1, pp 445453, Madrid
22. St John H.D. (1975). Field and theoretical of behavior of round around deep excavations in London City. PhD thesis, Universit f Cambridge
23. Wroth C.P. (1975). In-situ measurement of initial stresses and deformation characteristics. In Proc. Geot. Engng Div Speciality Conf. on In-situ Measurement of Soil Properties, pp 181-230, Rayleigh, NC, 1975. ASCE
24. Jardine, R. J., Symes, M. J. & Burland, J. B. (1984). The measurement of soil stiffness in the triaxial apparatus. Geotechnique 34, No. 3, 323-340. DOI: 10.1680/geot.1984.34.3.323
25. Jardine, R.J., Potts, D.M., Fourie, A.B., Burland, J.B., (1986). Studies of the influence of non-linear stress-strain characteristics in soil-structure interaction. Geotechnique, vol. 36(3), pp. 377-396, ISSN 0016-8505.
26. Jardine, R.J. (1992). Some observations on the kinematic nature of soil stiffness. Soil and Foundations, vol.32, n 2, 111-124, June 1992. Japanese Society of Soil Mechanics and Foundation Engineering
27. Arkinsos J.H., Sallfors G. (1991). Experimental determination of soil properties. In Proc. 10th ECSMFE, vol. 3, pp 915-956, Florence. General report to Session 1
28. Mair R.J. (1993). Developments in geotechnical engineering research: application to tunnels and deep excavations. Proceedings of Institution of Civil Engineers, Civil Engineering, pp 27-41. Unwin Memorial Lecture 1992
29. Tatsuoka F. (2000). Impacts n geotechnical engineering of several recent findings from laboratory stress-strain tests on geomaterials. Department of Civil Engineering Mechanics, Columbia University. The 2000 Burmister Lecture
30. Benetatos C., Rocca V., Sacchi Q., Verga F. (2015) How to approach subsidence evaluation for marginal fields: a case History. Open Petrol Eng J, vol. 8, 2015, Pages 214-234, ISSN: 18748341. DOI: 10.2174/1874834101508010214
31. Giani G.P., Gotta A., Marzano F., Rocca V. (2017) How to Address Subsidence Evaluation for a Fractured Carbonate Gas Reservoir Through a Multi-disciplinary Approach. Geotechnical and Geological Engineering, vol. 35, issue 6, 1 December 2017, pp 2977-2989, DOI 10.1007/s10706-017-0296-7
32. Giani G., Orsatti S., Peter C., Rocca V. (2018). A Coupled Fluid Flow—Geomechanical Approach for Subsidence Numerical Simulation. Energies 2018, 11, 1804; doi: 10.3390/en11071804
33. Teatini P., Castelletto N., Ferronato M., Gambolati G., Janna C., Cairo E., Marzorati D., Colombo D., Ferretti A., Bagliani A., Bottazzi F. (2011). Geomechanical response to seasonal gas storage in depleted reservoirs: A case study in the Po River basin, Italy. Journal of geophysical research, vol. 116, F02002, doi:10.1029/2010JF001793, 2011
34. Castelletto N., Ferronato M., Gambolati G., Janna C., Teatini P., Marzorati D., Cairo E., Colombo D., Ferretti A., Bagliani A., Mantica S. (2010). 3D geomechanics in UGS projects. A comprehensive study in northern Italy. Copyright 2010 ARMA, American Rock Mechanics Association. This paper was prepared for presentation at the 44th US Rock Mechanics Symposium and 5th U.S.-Canada Rock Mechanics Symposium, held in Salt Lake City, UT June 27–30, 2010.
35. Darendeli M.B. (2001) Development of new family of normalized modulus reduction and material damping reduction curves. PhD thesis, University of Texas at Austin.
36. Seed H.B., Idriss I.M. (1970). Soil moduli and damping factors for dynamic response analysis. Report 70-10, EERC, Berkeley, CA
37. Vermeer P.A. (1979) A modified initial strain method for plasticity problems. In Proc 3th Int. Conf. Numer. Meth. Geomech., pp 377-387. Balkema, Rotterdam
38. Benz T. (2007) Small-strain stiffness for soils and its numerical consequences. PhD Thesis, Institut fur Geotechnik der Universitat Stuttgart, Germany. Editor: Prof. Dr. Ing. P.A. Vermeer. ISBN 978-3-921837-55-9
39. Cadu M, Giraudi A., Rocca V, Verga F. (2012) Experimental laboratory tests focused on rock characterization for mechanical excavation. International Journal of Mining, Reclamation and Environment. vol. 26, issue 3, September 2012, pp 199-216. DOI: 10.1080/17480930.2012.712822.
40. Ghielmi M., Nini C., Livraghi L., Minervini M., Rogledi S., Rossi M., Sules O., Visentin C. (2008) Modern Po Plain-Adriatic Foredeep (Italy): Geological Framework and Hydrocarbon Exploration. 70th EAGE Conference & Exhibition Workshop, Rome (Italy), 8 June 2008.
41. Tran, D., Nghiem, L., Buchanan, L. (2005). An Overview of Iterative Coupling between Geomechanical Deformation and Reservoir Flow. SPE International Thermal Operations and Heavy Oil Symposium, Calgary, Alberta, Canada, 1-3 November 2005.
42. Ferronato M., Gambolati G., Teatini P. (2003). Unloading-reloading uniaxial compressibility of deep reservoirs by marker measurements. 11th FIG Symposium on Deformation Measurements, Santorini, Greece, 2003.
43. Teatini P., Castelletto N., Ferronato M., Gambolati G., Janna C., E. Cairo, Marzorati D., Colombo D., Ferretti A., Bagliani A., Bottazzi F. (2011) Geomechanical response to seasonal gas storage in depleted reservoirs: A case study in the Po River basin, Italy. Geophysical Research, 116, 2011.
44. Foti S. (2015). Comportamento dinamico dei terreni e prove di laboratorio. University Lecture.
45. 2Mayne P.W. (2000) Enhanced geotechnical site characterization by seismic piezocone penetration tests. Invited Lecture, Fourth International Geotechnical Conference, Cairo University, January 2000, pp. 95-120.
46. Geertsma, J. (1973a). Land subsidence above compacting oil and gas reservoirs. Journal of Petroleum Technology, vol. 25 (6), pp. 734-744.

47. Geertsma, J. (1973b). A basic theory of subsidence due to reservoir compaction: the homogeneous case. Verhandenlingen van het Koninklijk Nederlands Geologish Mijnbouwkundig Genootschap, vol. 28, pp. 43-72.
48. Berardino, P., Costantini, M., Franceschetti, G., Iodice, A., Pietranera, L., Rizzo, V. (2003). Use of differential SAR interferometry in monitoring and modelling large slope instability at Maratea (Basilicata, Italy). Eng. Geol. 2003, 68, 31–51.
49. Ferretti A., Prati C., Rocca F. (2001). Permanent scatterers in SAR interferometry. IEEE Trans. Geosci. Remote Sens. 2001, 39, 8–20.